

# Testing the drivers of the temperature–size covariance using artificial selection

Martino E. Malerba<sup>1,2</sup>  and Dustin J. Marshall<sup>1</sup> 

<sup>1</sup>Centre of Geometric Biology, School of Biological Sciences, Monash University, Melbourne, Victoria 3800, Australia

<sup>2</sup>E-mail: [martino.malerba@monash.edu](mailto:martino.malerba@monash.edu)

Received May 13, 2019

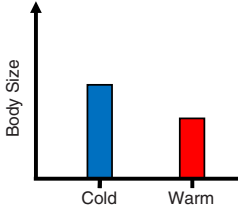
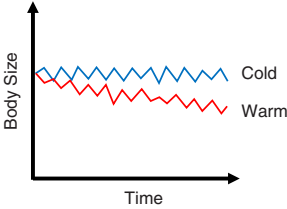
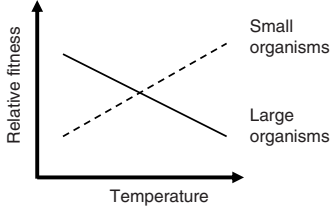
Accepted November 12, 2019

Body size often declines with increasing temperature. Although there is ample evidence for this effect to be adaptive, it remains unclear whether size shrinking at warmer temperatures is driven by specific properties of being smaller (e.g., surface to volume ratio) or by traits that are correlated with size (e.g., metabolism, growth). We used 290 generations (22 months) of artificial selection on a unicellular phytoplankton species to evolve a 13-fold difference in volume between small-selected and large-selected cells and tested their performance at 22°C (usual temperature), 18°C (–4), and 26°C (+4). Warmer temperatures increased fitness in small-selected individuals and reduced fitness in large-selected ones, indicating changes in size alone are sufficient to mediate temperature-dependent performance. Our results are incompatible with the often-cited geometric argument of warmer temperature intensifying resource limitation. Instead, we find evidence that is consistent with larger cells being more vulnerable to reactive oxygen species. By engineering cells of different sizes, our results suggest that smaller-celled species are pre-adapted for higher temperatures. We discuss the potential repercussions for global carbon cycles and the biological pump under climate warming.

**KEY WORDS:** Bergmann's rule, centre for geometric biology, chlorophyta, intraspecific size-scaling, phytoplankton green microalgae, temperature–size rule.

Body size covaries with most major characteristics of a species (Peters 1983; Roy 2008; Ginzberg et al. 2015). For example, population growth rates, mortality rates, generation time, and carrying capacity all covary with size (Brown et al. 2004). Among both ectothermic and endothermic organisms, an important driver of size at all levels of biological organization is temperature. Within species body sizes decrease with warmer climates (Bergmann 1847; Ashton 2002) and even within populations individuals exposed to higher temperatures are typically smaller than those exposed to lower temperatures (see Fig. 1A; Partridge et al. 1994; Atkinson et al. 2003; Fischer and Karl 2010). As global temperatures rise, concurrent reductions in body size have been labeled a “universal response to warming” (Gardner et al. 2011). Given the importance of body size for fitness and other eco-evolutionary parameters of a species, it is important to understand the ultimate drivers of covariation between body size and temperature (Walters and Hassall 2006).

Today, there is ample support that the negative covariance between body size and temperature is adaptive (but see Stillwell 2010). For instance, populations from locations with different temperatures often maintain their size differences after experiencing at least a generation of common garden conditions—ants (Heinze et al. 2003), snails (Gustafson et al. 2014), copepods (Lonsdale and Levinton 1985), and *Drosophila melanogaster* (Gilchrist and Patridge 1999; see review by Patridge and Coyne 1997). Moreover, trends in size across temperatures are similar in different continents, hold across latitudinal and altitudinal clines, and originate rapidly after the colonization of new habitats (Capy et al. 1994; Imasheva et al. 1994; Partridge and Coyne 1997; Huey et al. 2000). Finally, and most importantly, studies exposing laboratory lineages to thermal selection consistently generate bigger organisms at colder temperatures (see Fig. 1B; Partridge et al. 1994; Fischer and Karl 2010; Schlüter et al. 2014).

Question:	(A) Does temperature affect size?	(B) Does temperature select for reduced size?	(C) Does temperature affect size dependent fitness?
Methods:	Measure size of organisms exposed to different temperatures	Evolve organisms at different temperatures and monitor size over time.	Engineer genetic differences in body size and quantify fitness across temperatures.
Results:			
Inferences:	Determines if body size changes in response to temperature, but not if such responses are adaptive.	Determines if different temperatures favor different sizes, but not if size or other traits correlated to size (e.g. metabolism) are under selection.	Determines if body size causes different fitness returns under different temperatures, but cannot inform on other traits also favored across temperatures.
E.g.:	Atkinson 1994	Schlüter et al 2014	This study

**Figure 1.** Schematic of the main approaches used to investigate the negative covariance between temperature and body size. Initially, research focused on documenting trends between temperature and body size among species (question A). Later work used experimental evolution to test if size reductions represent an adaptive phenotypic plasticity (question B). By using artificial selection on a common ancestor to evolve lineages with different body sizes (while controlling for biotic and abiotic variables), our work investigates the active involvement of body size in determining the size-dependent fitness across temperatures (question C).

While the effects of temperature on body size have been investigated extensively, considerable controversy still exists regarding the underlying mechanisms. In particular, it is unclear as to whether size or other size-related traits are the target of temperature effects (Angilletta et al. 2003; Angilletta et al. 2004). For example, smaller sizes may be favored at warmer temperatures because of specific properties of being smaller (e.g., higher surface to volume ratio; Van der Have and De Jong 1996; Woods 1999; Stillwell et al. 2008). Alternatively, body size may coevolve with temperature through other traits that actually respond to temperature and are genetically correlated with size (constrained evolution of correlated traits; e.g., Lande 1979). For example, it is easy to imagine higher mass-specific metabolic rates, or higher relative growth rates being favored under higher temperatures, both of which typically negatively covary with size (Brown et al. 2004). As such, it is possible that size may simply covary with the actual target of selection under different temperature regimes.

Identifying which traits are directly under selection across temperature regimes is complex. For instance, traditional approaches of manipulating temperatures and examining the evolution of the size of a species are not necessarily causative. A wide range of correlated physiological, morphological, and life-history traits change simultaneously across temperatures, which prevent establishing a direct link between body size and fitness. Using populations of different sizes from different geographic locations is equally problematic, because those lineages are likely to differ in a wide range of potentially confounding traits that will also affect their response to temperature. One solution is to turn this problem on its head—manipulate the body size of a com-

mon ancestor and examine its size-dependent fitness under different temperatures (see Fig. 1C). This approach is labor-intensive, but allows determining whether differences in size alone affect fitness under different temperature regimes. Such studies have been restricted to a few model metazoans and provide ambivalent evidence for an interaction between body size selection and environmental temperature. For example, artificial selection on body size influenced fitness across temperatures in *Drosophila melanogaster* (McCabe and Partridge 1997; Reeve et al. 2000; Trotta et al. 2007) and yellow dung flies (Teuschl et al. 2007), but not in seed beetles (Stillwell et al. 2008). Therefore, the role of body size in mediating temperature-dependent fitness remains largely unresolved, especially for unicellular organisms.

To isolate if and how body size per se affects the performance of a species at different temperatures, we used 290 generations (22 months) of artificial selection to genetically engineer a 13-fold difference in mean body size between small- and large-selected phytoplankton lineages of the unicellular green microalga (*Dunaliella tertiolecta*). After that, we exposed lineages to different temperatures to evaluate the short-term fitness among phenotypes of varying body sizes. If body size plays a direct role in the temperature-size negative covariance, we would expect small-selected lineages to better cope with increasing temperatures compared to large-selected lineages (Fig. 1). In this case, we would also expect greater size plasticity among larger lineages at higher temperatures, as these organisms would be suffering the greatest fitness penalty. To this end, we took 36 independent lineages across a factorial design of three artificial selection treatments (small-selected, large-selected, and control) and three

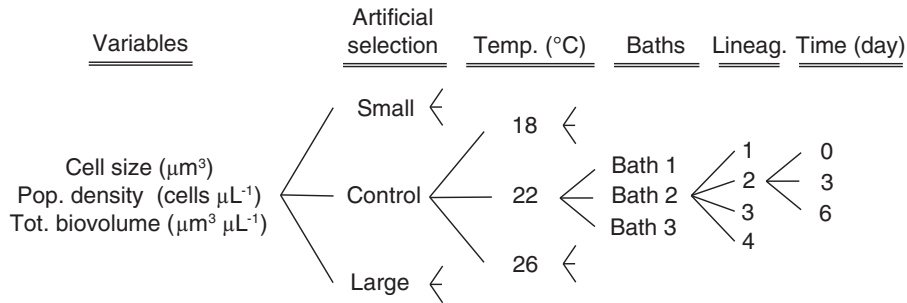


**Figure 2.** Experimental design. Three variables were monitored across a factorial design of three artificial selection treatments (i.e., small-selected, large-selected, and control), three temperatures (18, 22, and 26°C), three independent temperature baths, each containing four independent lineages that were monitored at day 0, 3, and 6 after inoculation (972 observations).

temperatures (18, 22, 26°C), each monitored for mean cell size, population density, and total biovolume for a week (972 observations; see Fig. 2 for experimental design). From there, we analyzed the effects of temperature at each artificial selection treatment on mean cell size and three fitness proxies (i.e., rate of cell production, rate of biovolume production, population carrying capacity).

Our results showed that small-selected cells have higher performance at warmer temperatures than cooler temperatures, while large-selected cells show the opposite pattern. One explanation for our results is that warmer temperatures exacerbate the negative effect of resource-limitation associated with larger organisms, and their smaller surface area to volume ratio (Agawin et al. 2000; Marañón et al. 2012). To test this mechanism, we compared temperature effects under high resource conditions (from day 0 to day 3) and low resource conditions (from day 3 to day 6) at each size-selection treatment. We find no evidence for resource limitation driving our result. Instead, we find support for an alternative explanation that oxidative stress leads to greater reactive oxygen species (ROS) accumulation inside larger cells (Suzuki and Mittler 2006).

## Materials and Methods

### STUDY SPECIES AND CULTURING CONDITIONS

As a model species, we chose the green microalgal species *Dunaliella tertiolecta* (Butcher) because it is cosmopolitan, tolerates a wide range of climates (from tropical to subpolar), has an intermediate body size compared to other phytoplankton species, and grows well in the laboratory (Guiry et al. 2019). We sourced this species from the Australian National Algae Culture Collection (ANACC; strain code CS-14) and started cultures from multiple cells per independent lineage (i.e., not clonal), cultured in autoclaved F/2 medium (with no silica) from 0.45  $\mu\text{m}$ -filtered seawater (Guillard 1975). We kept the environment constant using a temperature-controlled room at  $21 \pm 1^\circ\text{C}$ , under a photoperiod of 14–10 h day–night and a light intensity of 150  $\mu\text{M}$  photons

$\text{m}^{-2} \text{s}^{-1}$ , using low-heat 50 W LED flood lights (Power-lite™, Nedlands Group, Bedforddale, Australia).

### ARTIFICIAL SELECTION FOR SIZE

For details on the artificial selection methods, see Malerba et al. (2018c). Briefly, the method relies on larger cells forming a pellet at the bottom of test tubes at lower centrifugal forces compared to smaller cells, which instead will remain in solution (i.e., differential centrifugation). On April 25, 2016, we inoculated 72 lineages with the same ancestral population of *D. tertiolecta* into aseptic 75  $\text{cm}^2$  plastic cell culture flasks (Corning, Canted Neck, Nonpyrogenic). Since then, we selected lineages twice a week, each Monday and Thursday: 30 lineages were large-selected, 30 small-selected, and 12 were the control. The selection differential for both larger and smaller cells was approximately 10% shift between cell volume before and after artificial selection. Control cultures experienced identical conditions (including centrifugation) without being size-selected. At the end of selection, all cultures were diluted approximately three to five times in fresh F/2 medium. Lineages were not axenic, but we kept bacterial loads to minimal levels by resuspending pelleted cells in autoclaved medium twice a week and by handling samples using sterile materials under a laminar-flow cabinet (Gelman Sciences Australia, CF23S, NATA certified).

For this experiment, we used cells sampled from 12 randomly selected lineages for each of the three size-selection treatments after 290 generations (22 months) of artificial selection. To remove any environmental effects and nongenetic phenotypic differences from artificial selection, before starting trials all cells grew for three generations (a week) under common garden conditions with no centrifugation (i.e., unselected transfer). Following the unselected transfer, we measured the mean cell volume for all 36 lineages, using optic light microscopy at 400 $\times$  after staining cells with lugol's iodine at 2%. We calculated cell volume from at least 200 cells per culture in Fiji v2.0 (Schindelin et al. 2012) assuming prolate spheroid shape, as recommended for this species by Sun and Liu (2003).

### TEMPERATURE TRIALS

After the unselected transfer at  $21 \pm 1^\circ\text{C}$ , we diluted samples from the 36 lineages 10-fold, resuspended into fresh F/2 medium, and standardized for initial total biovolume (i.e., population density  $\times$  mean cell volume; unit  $\mu\text{m}^3 \mu\text{L}^{-1}$ )—which is a better predictor for resource use than population density. We submerged all cultures inside transparent and side-illuminated water baths at a controlled temperature of either  $22^\circ\text{C}$  (usual temperature),  $18^\circ\text{C}$  ( $-4$ ), and  $26^\circ\text{C}$  ( $+4$ ; see Fig. 2 for experimental design). This temperature range mirrors usual yearly fluctuations in sub-tropical regions where this species is often found. Each temperature included three independent water baths, each holding 12 lineages (four per size-selection treatment; see Fig. 2). We manipulated the temperature of each water bath using a submersible aquarium heater placed behind the samples so as not to affect light exposure. We ensured that daily temperature fluctuations were within  $\pm 1^\circ\text{C}$ . The experiment took place in a temperature-controlled room and samples experienced identical light conditions of 14–10 h day–night photoperiod with a light intensity of about  $100 \mu\text{M}$  photos  $\text{m}^{-2} \text{s}^{-1}$ .

We monitored all samples for mean cell volume, population density, and total biovolume at day 0, 3, and 6. We recorded population density (i.e., cells  $\mu\text{L}^{-1}$ ) with a flow cytometer (FlowCore, BD LSRII; BD Biosciences, Franklin Lakes, NJ, USA) using a blue laser (488 nm) and CountBright absolute counting beads (Thermo Fisher, Waltham MA, USA) as internal standards in each sample. We inferred the mean cell volume ( $\mu\text{m}^3$ ) of a population using a calibration curve between the mean of the cytometric histogram for the forward scatter (after standardizing for the mean of the beads) and the mean cell volume measured using optical light microscopy ( $R^2 = 0.84$ ,  $F_{1,106} = 540.9$ ,  $P < 0.001$ ). Finally, we calculated the total biovolume ( $\mu\text{m}^3 \mu\text{L}^{-1}$ ) by multiplying the population density by the mean cell volume. In total, the dataset included 972 observations (3 artificial selections  $\times$  3 temperatures  $\times$  3 baths  $\times$  4 replicates  $\times$  3 times  $\times$  3 demographic parameters).

### ROS ASSAYS

We adopted the methods for quantifying intracellular ROS from Dao and Beardall (2016). After three generations of no centrifugation, we standardized six lineages per size-selection treatment to the same total biovolume and washed all populations three times into saline 40 mM TRIS-HCl buffer (pH 7 and 35 ppt). Then, we dark-incubated cells in  $50 \mu\text{M}$  of fluorescent probe 2',7'-dichlorodihydrofluorescein diacetate (DCFH-DA) for 90 min at  $37^\circ\text{C}$ . After resuspending the pellet in buffer, we sonicated cells for 10 min. We measured the fluorescence of the supernatant in a spectrophotometer (Hitachi F-7000, Tokyo, Japan) at wavelengths of 485 nm (excitation) and 525 nm (emission). Values were converted into fluorescence units of dichloro-fluorescein

(nM) using a 7-point calibration curve (second degree polynomial:  $R^2 = 0.999$ ). The buffer was the negative control and dichlorofluorescein (DCF) from 5 to 75 nM was the positive control. We standardized ROS fluorescence in a sample for cell density and for the volume of the cell's nucleus. Nucleus size was estimated from fluorescent microscopy (excitation at 325–375 nm and emission at 435–485 nm) with Leica DMi8 at  $400\times$  after fixing cells with 2% glutaraldehyde and resuspending the biomass in DAPI at  $0.1 \mu\text{g mL}^{-1}$ . The allometric relationship was:  $\log_{10} \text{ nucleus volume} = 0.479 \times \log_{10} \text{ cell volume} - 0.122$ .

### DATA ANALYSIS

We calculated three parameters that estimate the species short-term fitness from each time-series. The daily cell production (cells  $\mu\text{L}^{-1} \text{ day}^{-1}$ ) of a lineage indicates rate of change in population densities between day 0 and 3. The daily biovolume production ( $\mu\text{m}^3 \mu\text{L}^{-1} \text{ day}^{-1}$ ) is the slope of total biovolume between day 0 and day 3. The population carrying capacity (cells  $\mu\text{L}^{-1}$ ) was the final cell density of each lineage after the time-series reached a stable state (6 days). Finally, we analyzed the effects of temperature on mean cell volumes ( $\mu\text{m}^3$ ) between day 0 and day 3 among size-selection treatments.

We used linear mixed models to estimate the effects of temperature at each artificial selection treatment on mean cell size and the three fitness parameters. In all models, fixed effects included “Temperature” (continuous, from 18 to  $26^\circ\text{C}$ ) and “Artificial Selection Treatment” (discrete, either small-selected, large-selected, or control). We ensured that treating Temperature as a discrete categorical factor did not change any of the conclusions (see Fig. S1). For mean cell size, we monitored cultures for 6 days: to focus on phenotypic plasticity and exclude evolutionary effects, we only analyzed observations at the start of the experiment and after 3 days of growth, with “Time” (continuous, from 0 to 3 days) as an additional fixed factor in the model. Initial models included all interaction terms. If not significant, higher-order interaction terms were removed from the model. Final models also included a random intercept for each lineage nested within treatment. We initially included a random slope with temperature, but that was later removed from the final models after being consistently selected against by model selection with Akaike Information Criterion (Burnham and Anderson 2002). We calculated probability values for the linear mixed-models using an analysis of deviance with type II Wald chi-square test and Kenward–Roger approximation to calculate the degrees of freedom (see Table S1).

We carried out all analysis and plotting in R version 3.5.0 (R Core Team 2018) using packages nlme (Pinheiro et al. 2016), lme4 (Bates et al. 2015), plyr (Wickham 2011), car (Fox and Weisberg 2019), and ggplot2 (Wickham 2009).

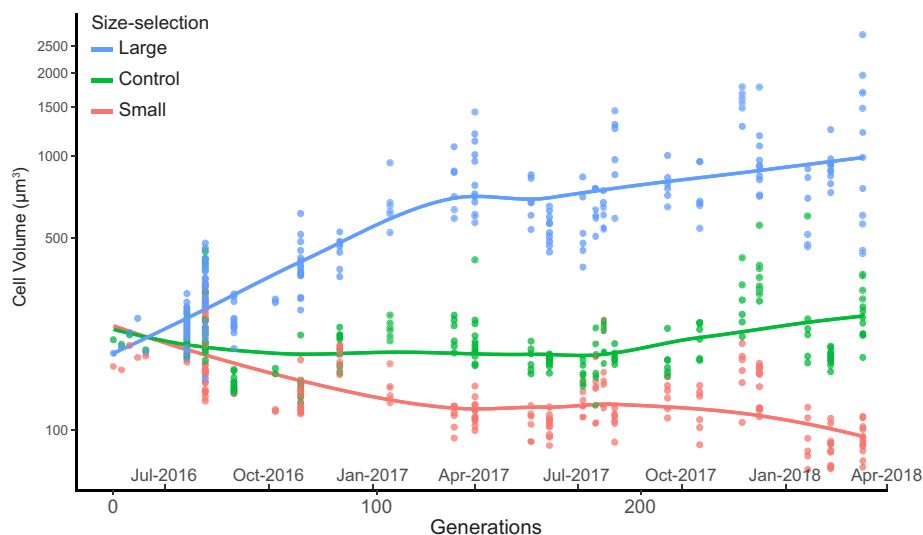


**Figure 3.** Effects of two years of artificial size-selection (about 300 generations) on the cell volume of *D. tertiolecta*. Each point represents the mean cell volume of an independent lineage after measuring c. 200 cells per lineage. Lines indicate the fit of a LOESS smoother for each size-selection treatment (either small-selection, large-selection, or control). Temperature trials were conducted after 290 generations (22 months) using 12 randomly sampled lineages for each size-selection treatment and the mean cell volume was  $93.2 (\pm 3.5 \text{ SE})$ ,  $272.3 (\pm 16.8)$ , and  $1217.3 (\pm 207.8) \mu\text{m}^3$  for small, control and large, respectively.

## Results

### CELL SIZE EVOLUTION

After 290 generations of artificial selection, the mean volume of large-selected cells ( $1217.3 \pm 207.8 \text{ SE}$ ) was 4.5 times larger than control cells ( $272.3 \pm 16.8$ ) and 13 times larger than small-selected cells ( $93.2 \pm 3.5$ ; Fig. 3). On average, the mean cell volume increased by 0.6% per generation in large-selected lineages (linear regression:  $F_{1,25} = 116.31$ ,  $P < 0.001$ ), and decreased by 0.2% in small-selected lineages ( $F_{1,25} = 23.367$ ,  $P < 0.001$ ). Control lineages did not show any trend in size over time ( $F_{1,24} = 2.36$ ,  $P = 0.14$ ; Fig. 3).

### TEMPERATURE EFFECTS ON PRODUCTIVITY RATES

Small-selected cells increased productivity—both per biovolume (Fig. 4A) and per cell (Fig. 4B)—with increasing temperatures, whereas large-selected cells showed the opposite trend. Control lineages were intermediate, with no statistical support for an effect of temperature (i.e., coefficient largely overlapping 0; see Fig. 4A and 4B for coefficients and Fig. S2 for model fits). Rates of daily biovolume production increased more than doubled (+108%) in small-selected lineages from 18 to 26°C (positive slopes in Fig. 4A). Instead, the same temperature gradient led to a decrease in biovolume production for large-selected (−79%) lineages (negative slopes Fig. 4A). Similarly, rates of daily cell production increased with increasing temperatures in small-selected lineages (+48%), while mostly decreased in large-selected lineages (−37%) and showed no effect of temperature in Control lineages (Fig. 4B).

### TEMPERATURE EFFECTS ON POPULATION CARRYING CAPACITY

The population carrying capacity after 6 days of growth increased with temperature in small-selected (+42%) and control lineages (+48.5%), and decreased with temperature in large-selected lineages (−37%; Fig. 4C and Fig. S2 for model fits).

### TEMPERATURE EFFECTS ON MEAN CELL SIZE

Size-selection treatments showed different effects of temperature on the mean cell size within the population (Table S1). Control cells showed the greatest temperature sensitivity during the experiment, decreasing in volume by up to 40% between 18 and 26°C. Conversely, small- and large-selected cells showed little change in mean cell size across temperature (both slopes overlapping 0 in Fig. 4D; see Fig. S2 for model fits). Moreover, all populations recorded larger mean cell sizes at the beginning of the experiment (day 0) compared to the end (day 6; see Fig. S3).

### TEMPERATURE EFFECTS ACROSS RESOURCE LEVELS

The specific growth rate of all lineages decreased considerably between days 0 to 3 and days 3 to 6 (see Fig. S4), indicating that cultures became increasingly more resource limited. If warmer temperatures exacerbate resource limitation more in larger cells than smaller ones, we would expect different temperature effects between growth under high resources (from day 0 to day 3) and low resources (from day 3 to day 6) at each size-selection treatment. Instead, all temperature effects on biomass and cell productivity remained comparable between resource-replete exponential

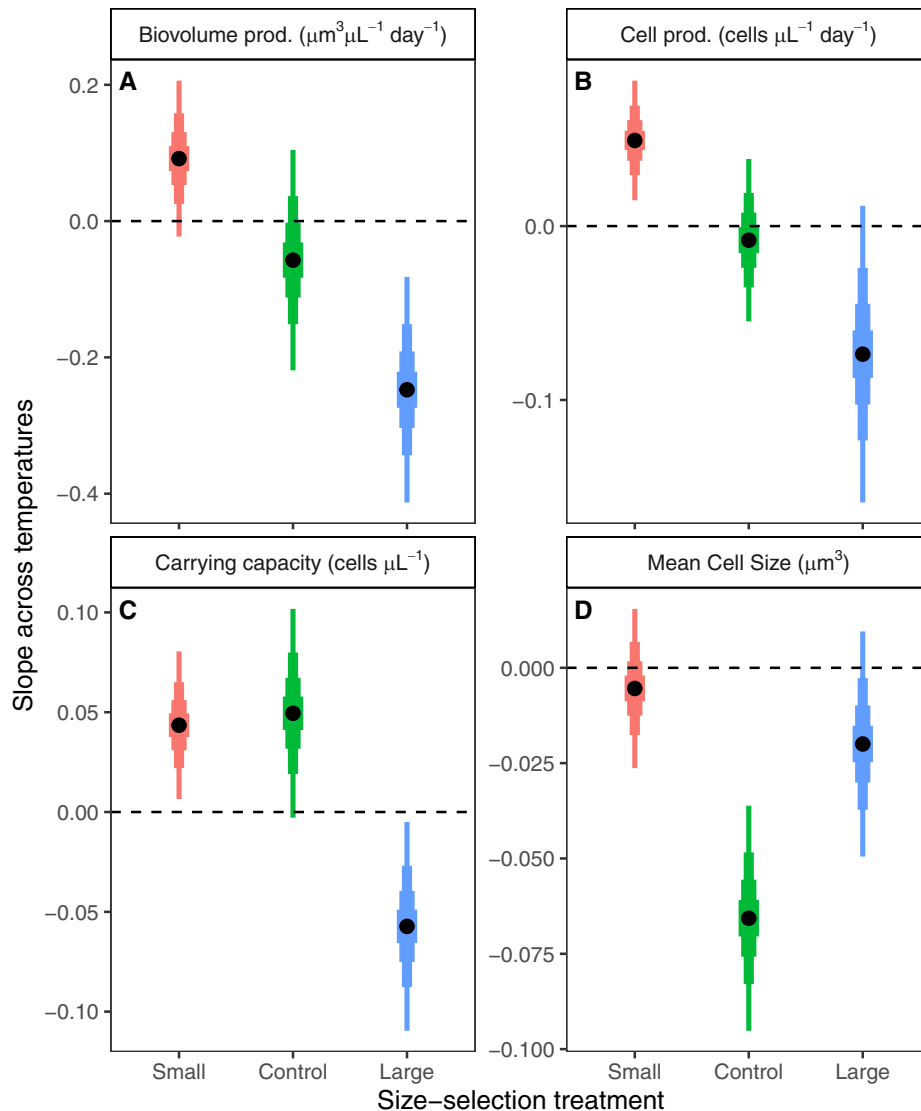


**Figure 4.** Mean temperature sensitivity between 18 and 26°C for demographic parameters among artificial selection treatments. Slopes were extracted from the best-fitting linear mixed-model. A positive slope represents a positive effect of temperature on the demographic parameter, and vice-versa. Each coefficient is color-coded for the artificial selection treatment and is partitioned into quantiles representing 95%, 75%, 50%, and 25% of the distribution. See Fig. S2 for all model fits and Table S1 for ANOVA tables.

growth phases and at the onset of stationary phase and resource limitation (Fig. S5).

#### ROS ASSAY

If size-dependent fitness across temperature is mediated by ROS toxicity, we would expect different relative intracellular ROS levels among size-selected lineages. Results show that large-selected cells have 4.7 times more ROS than small-selected cells (Fig. 5A). Moreover, larger cells have two times more ROS when standardized for their nucleus volume compared to small-selected cells (Fig. 5B). Finally, there was no statistical difference in ROS levels among size treatments when standardizing for cell biovolume ( $F_{2,15} = 2.12$ ,  $P = 0.154$ ; data not shown).

#### Discussion

By using artificial selection to evolve different cell sizes, our results showed that body size per se can directly affect the short-term performance of a species across temperatures. Warmer temperatures increased fitness in small-evolved individuals and reduced fitness in large-evolved individuals. Hence, our results demonstrate that some intrinsic property of body size determines the temperature-dependent fitness of an organism.

Our results showed that smaller cells benefitted from higher temperatures, but they did not provide insight as to why. It has long been argued that smaller cells are better in warmer temperatures because they have a greater surface to volume ratio. All else being equal, cells assimilate light and nutrients

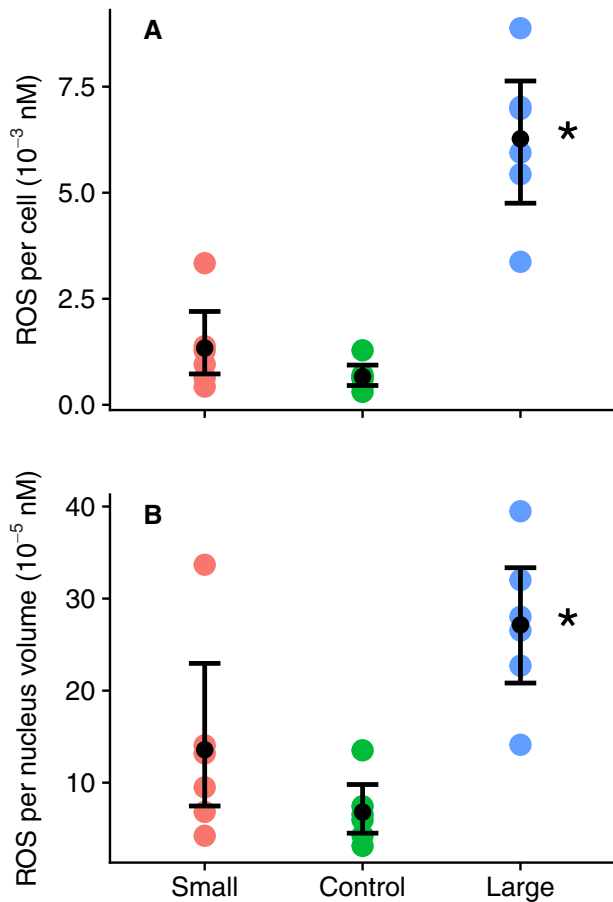


**Figure 5.** Intracellular reactive oxygen species (ROS) for each size-selection treatment calculated (A) per unit cell and (B) per unit cell's nucleus volume. Asterisks indicate significant differences following linear models and Tukey's post-hoc test. ROS concentrations are expressed as fluorescence units of dichloro-fluorescein. Note that there was no statistical difference in ROS per biovolume among size treatments ( $F_{2,15} = 2.12$ ,  $P = 0.154$ ; data not shown).

proportionally to surface area, which scales at two thirds of cell volume. Conversely, resource consumption is roughly proportional to volume (Aksnes and Egge 1991; Okie 2013; Maranon 2015). Under these geometrical assumptions, as cell size increases, resource uptake from increasing surface area should increase more slowly than resource consumption (Niklas 2013). While there is variation in temperature sensitivity among enzymes (Padfield et al. 2016; Schaum et al. 2018), warmer temperatures generally accelerate the cell's enzyme reactions and protein synthesis, perhaps increasing resource demands to rates that cannot be met by larger cells with (relatively) small surface to volume ratios. Hence, theory predicts that organisms reduce their body size to increase their surface to volume ratio and better cope with the increased demands associated with warmer temperatures on resource assimilation (Atkinson et al. 2006; Sommer et al. 2017). Support for this theory comes from studies that suggest low re-

sources intensify temperature-dependent effects on larger species (Rhee and Gotham 1981; Persson et al. 2011; Cross et al. 2015).

Our results were incompatible with the explanation that warmer temperatures exacerbate resource limitation in larger cells. If resources were driving temperature effects, we would expect larger cells to suffer greater costs later in the experiment at higher population densities, when light, nutrients, and other resources are less available. Instead, all temperature effects on population fitness remained equivalent between resource-replete (days 0–3) and at the onset of resource limitation (days 3–6). Furthermore, populations of large cells still maintained positive growth at warm temperatures, rejecting the hypothesis that resource limitation (e.g., oxygen, *sensu* Woods 1999) could act as an absolute constraint on body size. Perhaps, cells evolving to larger sizes also developed strategies to assimilate resources while minimizing geometrical constraints. For example, we showed that large-selected cells modified their photosynthetic apparatus, by evolving smaller light-harvesting antennae and greater pigments densities (Malerba et al. 2018a). Although in nature larger cells are typically inferior competitors under low nutrients (Maranon 2015), it is likely that our lineages have evolved systems for nutrient uptake and distribution to compensate for the geometrical constraints of increasing volumes. While we have no data on nutrient utilization among size-evolved lineages, present evidence suggests that the mechanisms driving the size-dependent temperature response in this species are more complex than the often-cited geometrical arguments on surface to volume ratios.

Instead, we find evidence for ROS driving our results. An increase in temperature will increase the electron flow of photosynthetic cells and make them more susceptible to light-induced damage (Vacca 2004; Suzuki and Mittler 2006). A well-known effect of exceeding photosynthetic capacity is the leakage of electrons onto  $O_2$  by the electron transport chain, thereby generating ROS (Key et al. 2010). When cells are unable to downregulate photosynthetic energy, oxidative stress from ROS accumulation can reduce the performance of a cell, mostly through DNA damages (Suzuki and Mittler 2006). Our previous studies on this model system suggest that large-selected cells may be more vulnerable to ROS toxicity than small-selected cells. First, large-selected cells have much faster energy rates than smaller cells (+899% per-cell and +69% per-volume; Malerba et al. 2018a; Malerba and Marshall 2019) hence, greater potential to generate ROS. Second, beta-carotene is a key photo-protectant pigment against ROS and its mass-specific density is 55% lower in large-selected cells than smaller ones (Malerba et al. 2018a). Third, the sensitivity to photodamage is proportional to Chlorophyll-a concentration among phytoplankton species (Echeveste et al. 2011) and its mass-specific density is 61% greater in large-selected cells (Malerba et al. 2018a). Consistent with expectations, we found that our larger cells have almost five times more ROS than smaller

cells. Furthermore, larger cells have disproportionately smaller nuclei, leading to twice as much ROS loads around their nucleus than smaller cells (but notice that all sizes had equivalent ROS per biovolume). While these results cannot attribute causality, they are consistent with the hypothesis that ROS toxicity may explain size-dependent fitness across temperatures that are independent of nutrient levels. Also, if temperature effects are driven by size-dependent ROS toxicity, we would expect that other ROS-producing stressors (e.g., high irradiance) should favor smaller cells. However, such predictions are complicated by the fact that photosystems and ROS-absorbing pigments coevolved with cell size in this species (Malerba et al. 2018a). In the future, we hope to test our hypothesis on ROS toxicity by verifying that costs to larger sizes intensify at higher light levels.

We found evidence for differences in temperature-induced phenotypic plasticity among our selection treatments. Control populations showed a 40% decrease in mean cell volume from 18 to 26°C, whereas small- and large-selected cells did not show any trend with temperature. In other words, unselected cells showed far greater potential for rapid phenotypic change in volume than size-evolved lineages. This is consistent with control cells increasing in volume twice as much as large- or small-selected cells under nutrient limitation (Malerba et al. 2018b). It is likely that the most extreme genotypes produced after nearly 300 generations of artificial selection are also the least plastic in body size. Our artificially selected lineages are under strong and constant selection pressures, which are predicted to generate specialized and monomorphic phenotypes with a reduced niche breadth and plasticity, relative to unselected (control) populations (Futuyma and Moreno 1988; DeWitt et al. 1998; Chevin and Hoffmann 2017).

## Conclusions

Organisms are becoming smaller in response to human activities, with phytoplankton species revealing some of the greatest declines in size in response to warming oceans (Atkinson et al. 2003; Gardner et al. 2011). Our results showed that cells evolving to smaller sizes may have an advantage under higher temperatures. But these adaptive changes may have worrying consequences for food web structures and global carbon cycles. For instance, smaller cells sink more slowly, which could reduce the efficacy of the biological carbon pump and the capacity of the ocean to act as a long-term sink for atmospheric carbon dioxide (Steinacher et al. 2010; Bopp et al. 2013) – although many cellular attributes other than cell size influence phytoplankton sinking rates (Richardson and Jackson 2007). This reduction in cell sinking may add to global warming by reinforcing thermal stratification and further reducing the flow of organic matter to the deep ocean.

By engineering cells of different sizes, we revealed new insights into the drivers of the negative correlation between body

size and temperature, which is so pervasive in biology. Our results showed that smaller sizes benefit from warmer temperatures and that there are aspects intrinsic to body size that confer these benefits. However, we found no support for the often-cited mechanism for why smaller cells might perform better at higher temperatures (i.e., increasing surface-area to volume ratios to cope with increased resource demand). Instead, our data support the hypothesis that size-dependent ROS accumulation drove our results. Further studies are necessary to determine whether our findings apply to other systems, in particular on how body size and ROS covary across temperatures in other organisms.

## AUTHOR CONTRIBUTIONS

All authors contributed to designing the study. MEM conducted the experiment, collected the data and carried out statistical analyses. MEM and DJM wrote the initial draft of the manuscript. Both authors gave final approval for publication.

## ACKNOWLEDGMENTS

We thank Tormey Reimer, Lucy Chapman and Dr Maria del Mar Palacios Otero for their help with laboratory procedures. We also thank Prof Don R. Levitan for insightful comments and suggestions. Thanks to Prof. John Beardall and Dr Yussi M. Palacios Delgado for their assistance with ROS assays. We would like to express our gratitude to Lesley Wiadrowski, Stewart Crowley and John Arvanitakis for logistical support at Monash University. Finally, we are particularly grateful to the Australian Research Council for financial support. The authors declare no conflict of interest.

## DATA ARCHIVING

The doi for this article is <https://doi.org/10.5061/dryad.wstqjq2gp>.

## LITERATURE CITED

- Agawin, N. S. R., C. M. Duarte, and S. Agustí. 2000. Nutrient and temperature control of the contribution of picoplankton to phytoplankton biomass and production. *Limnol. Oceanogr.* 45:591–600.
- Aksnes, D., and J. Egge. 1991. A theoretical model for nutrient uptake in phytoplankton. *Mar. Ecol. Prog. Ser.* 70:65–72.
- Angilletta, J., J. Michael, and A. E. Dunham. 2003. The temperature-size rule in ectotherms: simple evolutionary explanations may not be general. *Am. Nat.* 162:332–342.
- Angilletta Jr, M. J., T. D. Steury, and M. W. Sears. 2004. Temperature, growth rate, and body size in ectotherms: fitting pieces of a life-history puzzle. *Integr. Comp. Biol.* 44:498–509.
- Ashton, K. G. 2002. Patterns of within-species body size variation of birds: strong evidence for Bergmann's rule. *Glob. Ecol. Biogeogr.* 11:505–523.
- Atkinson, D., B. J. Ciotti, and D. J. Montagnes. 2003. Protists decrease in size linearly with temperature: ca. 2.5% C<sup>-1</sup>. *Proc. R. Soc. Lond. Ser. B. Biol. Sci.* 270:2605–2611.
- Atkinson, D., S. A. Morley, and R. N. Hughes. 2006. From cells to colonies: at what levels of body organization does the 'temperature-size rule' apply? *Evol. Dev.* 8:202–214.
- Bates, D., M. Maechler, B. Bolker, and S. Walker. 2015. Fitting Linear Mixed-effects models using lme4. *J. Stat. Softw.* 67:1–48.
- Bergmann, C. 1847. Ueber die Verhältnisse der Wärmeökonomie der Thiere zu ihrer Grösse (Concerning the relationship of heat conservation of animals to their size). *Göttinger Studien.* 3:595–708.

- Bopp, L., L. Resplandy, J. C. Orr, S. C. Doney, J. P. Dunne, M. Gehlen, P. Halloran, C. Heinze, T. Ilyina, R. Seferian, et al. 2013. Multiple stressors of ocean ecosystems in the 21st century: projections with CMIP5 models. *Biogeosciences* 10:6225–6245.
- Brown, J. H., J. F. Gillooly, A. P. Allen, V. M. Savage, and G. B. West. 2004. Toward a metabolic theory of ecology. *Ecology* 85:1771–1781.
- Burnham, K. P., and D. R. Anderson. 2002. Model selection and multimodel inference: a practical information-theoretic approach. Springer-Verlag New York.
- Capy, P., E. Pla, and J. David. 1994. Phenotypic and genetic variability of morphometrical traits in natural populations of *Drosophila melanogaster* and *D. simulans*. II. Within-population variability. *Genet. Select. Evol.* 26:15.
- Chevin, L. M., and A. A. Hoffmann. 2017. Evolution of phenotypic plasticity in extreme environments. *Philos. Trans. R. Soc. Lond. B Biol. Sci.* 372:20160138.
- Cross, W. F., J. M. Hood, J. P. Benstead, A. D. Huryn, and D. Nelson. 2015. Interactions between temperature and nutrients across levels of ecological organization. *Global Change Biol.* 21:1025–1040.
- Dao, L. H., and J. Beardall. 2016. Effects of lead on growth, photosynthetic characteristics and production of reactive oxygen species of two freshwater green algae. *Chemosphere* 147:420–429.
- DeWitt, T. J., A. Sih, and D. S. Wilson. 1998. Costs and limits of phenotypic plasticity. *Trends Ecol. Evol.* 13:77–81.
- Echeveste, P., S. Agusti, and J. Dachs. 2011. Cell size dependence of additive versus synergistic effects of UV radiation and PAHs on oceanic phytoplankton. *Environ. Pollut.* 159:1307–1316.
- Fischer, K., and I. Karl. 2010. Exploring plastic and genetic responses to temperature variation using copper butterflies. *Clim. Res.* 43:17–30.
- Fox, J., and S. Weisberg. 2019. An R companion to applied regression, 3rd edition. Sage, Thousand Oaks, CA. <https://socialsciences.mcmaster.ca/jfox/Books/Companion/>.
- Futuyma, D. J., and G. Moreno. 1988. The evolution of ecological specialization. *Annu. Rev. Ecol. Syst.* 19:207–233.
- Gardner, J. L., A. Peters, M. R. Kearney, L. Joseph, and R. Heinsohn. 2011. Declining body size: a third universal response to warming? *Trends Ecol. Evol.* 26:285–291.
- Gilchrist, A. S., and L. J. G. Partridge. 1999. A comparison of the genetic basis of wing size divergence in three parallel body size clines of *Drosophila melanogaster*. *Genetics* 153:1775–1787.
- Ginzberg, M. B., R. Kafri, and M. Kirschner. 2015. On being the right (cell) size. *Science* 348:1245075.
- Guillard, R. R. L. 1975. Culture of phytoplankton for feeding marine invertebrates. Pp. 26–60 in W. L. Smith, and M. H. Chanley, eds. Culture of marine invertebrate animals. Plenum Press, New York, USA.
- Guiry, M.D., and G. M. Guiry. 2019. AlgaeBase. World-wide electronic publication, National University of Ireland, Galway. <https://www.algaebase.org>; searched on 23 August 2019.
- Gustafson, K. D., B. J. Kensing, M. G. Bolek, and B. Luttbeg. 2014. Distinct snail (Physa) morphotypes from different habitats converge in shell shape and size under common garden conditions. *Evol. Ecol. Res.* 16:77–89.
- Heinze, J., S. Foitzik, B. Fischer, T. Wanke, and V. E. Kipyatkov. 2003. The significance of latitudinal variation in body size in a holarctic ant, *Leptothorax acervorum*. *Ecography* 26:349–355.
- Huey, R. B., G. W. Gilchrist, M. L. Carlson, D. Berrigan, and L. S. J. S. Serra. 2000. Rapid evolution of a geographic cline in size in an introduced fly. *Science* 287:308–309.
- Imasheva, A. G., O. A. Bubli, and O. E. Lazebny. 1994. Variation in wing length in Eurasian natural populations of *Drosophila melanogaster*. *Heredity* 72:508.
- Key, T., A. McCarthy, D. A. Campbell, C. Six, S. Roy, and Z. V. Finkel. 2010. Cell size trade-offs govern light exploitation strategies in marine phytoplankton. *Environ. Microbiol.* 12:95–104.
- Lande, R. 1979. Quantitative genetic analysis of multivariate evolution, applied to brain:body size allometry. *Evolution* 33:402–416.
- Lonsdale, D. J., and J. S. J. E. Levinton. 1985. Latitudinal differentiation in copepod growth: an adaptation to temperature. *Ecology* 66:1397–1407.
- Malerba, M. E., and D. J. Marshall. 2019. Size-abundance rules? Evolution changes scaling relationships between size, metabolism and demography. *Ecol. Lett.* 22:1407–1416.
- Malerba, M. E., M. M. Palacios, Y. M. P. Delgado, J. Beardall, and D. J. Marshall. 2018a. Cell size, photosynthesis and the package effect: an artificial selection approach. *New Phytol.* 219:449–461.
- Malerba, M. E., M. M. Palacios, and D. J. Marshall. 2018b. Do larger individuals cope with resource fluctuations better? an artificial selection approach. *Proc. Biol. Sci.* 285:20181347.
- Malerba, M. E., C. R. White, and D. J. Marshall. 2018c. Eco-energetic consequences of evolutionary shifts in body size. *Ecol. Lett.* 21:54–62.
- Maranon, E. 2015. Cell size as a key determinant of phytoplankton metabolism and community structure. *Annu. Rev. Mar. Sci.* 7:241–264.
- Marañón, E., P. Cermeño, M. Latasa, and R. D. Tardonléké. 2012. Temperature, resources, and phytoplankton size structure in the ocean. *Limnol. Oceanogr.* 57:1266–1278.
- McCabe, J., and L. Partridge. 1997. An interaction between environmental temperature and genetic variation for body size for the fitness of adult female *Drosophila melanogaster*. *Evolution* 51:1164–1174.
- Niklas, K. J. 2013. Biophysical and size-dependent perspectives on plant evolution. *J. Exp. Bot.* 64:4817–4827.
- Okie, J. G. 2013. General models for the spectra of surface area scaling strategies of cells and organisms: fractality, geometric dissimilitude, and internalization. *Am. Nat.* 181:421–439.
- Padfield, D., G. Yvon-Durocher, A. Buckling, S. Jennings, and G. Yvon-Durocher. 2016. Rapid evolution of metabolic traits explains thermal adaptation in phytoplankton. *Ecol. Lett.* 19:133–142.
- Partridge, L., B. Barrie, K. Fowler, and V. French. 1994. Evolution and development of body size and cell size in *Drosophila melanogaster* in response to temperature. *Evolution* 48:1269–1276.
- Partridge, L., and J. A. Coyne. 1997. Bergmann's rule in ectotherms: is it adaptive? *Evolution* 51:632–635.
- Persson, J., M. W. Wojewodzic, D. O. Hessen, and T. J. O. Andersen. 2011. Increased risk of phosphorus limitation at higher temperatures for *Daphnia magna*. *Oecologia* 165:123–129.
- Peters, R. H. 1983. The ecological implications of body size. Cambridge Univ. Press, Cambridge, U.K.
- Pinheiro, J., D. Bates, S. DebRoy, D. Sarkar, and R. Core Team. 2016. nlme: linear and nonlinear mixed effects models. R package version 3.1–128, <http://CRAN.R-project.org/package=nlme>.
- R Core Team. 2018. R: A language and environment for statistical computing. R Foundation for Statistical Computing, Vienna, Austria.
- Reeve, Fowler, and Partridge. 2000. Increased body size confers greater fitness at lower experimental temperature in male *Drosophila melanogaster*. *J. Evol. Biol.* 13:836–844.
- Rhee, G. Y., and I. Gotham. 1981. The effect of environmental factors on phytoplankton growth: temperature and the interactions of temperature with nutrient limitation. *Limnol. Oceanogr.* 26:635–648.
- Richardson, T. L., and G. A. Jackson. 2007. Small phytoplankton and carbon export from the surface ocean. *Science* 315:838–840.
- Roy, K. 2008. Dynamics of body size evolution. *Science* 321:1451–1452.
- Schaum, C.-E., A. Buckling, N. Smirnov, D. Studholme, and G. Yvon-Durocher. 2018. Environmental fluctuations accelerate molecular evolution of thermal tolerance in a marine diatom. *Nat. Commun.* 9:1719.

- Schindelin, J., I. Arganda-Carreras, E. Frise, V. Kaynig, M. Longair, T. Pietzsch, S. Preibisch, C. Rueden, S. Saalfeld, B. Schmid, et al. 2012. Fiji: an open-source platform for biological-image analysis. *Nat. methods* 9:676–682.
- Schlüter, L., K. T. Lohbeck, M. A. Gutowska, J. P. Gröger, U. Riebesell, and T. B. H. Reusch. 2014. Adaptation of a globally important coccolithophore to ocean warming and acidification. *Nat. Clim. Chang* 4:1024–1030.
- Sommer, U., K. H. Peter, S. Genitsaris, and M. Moustaka-Gouni. 2017. Do marine phytoplankton follow Bergmann's rule sensu lato? *Biol. Rev.* 92:1011–1026.
- Steinacher, M., F. Joos, T. Frölicher, L. Bopp, P. Cadule, V. Cocco, S. C. Doney, M. Gehlen, K. Lindsay, and J. K. Moore. 2010. Projected 21st century decrease in marine productivity: a multi-model analysis. *Biogeosciences* 7:979–1005.
- Stillwell, R. C. 2010. Are latitudinal clines in body size adaptive? *Oikos* 119:1387–1390.
- Stillwell, R. C., J. Moya-Larano, and C. W. Fox. 2008. Selection does not favor larger body size at lower temperature in a seed-feeding beetle. *Evolution* 62:2534–2544.
- Sun, J., and D. Y. Liu. 2003. Geometric models for calculating cell biovolume and surface area for phytoplankton. *J. Plankton Res.* 25:1331–1346.
- Suzuki, N., and R. Mittler. 2006. Reactive oxygen species and temperature stresses: a delicate balance between signaling and destruction. *Physiol. Plant* 126:45–51.
- Teuschl, Y., C. Reim, and W. U. Blanckenhorn. 2007. Correlated responses to artificial body size selection in growth, development, phenotypic plasticity and juvenile viability in yellow dung flies. *J. Evol. Biol.* 20:87–103.
- Trotta, V., F. C. Calboli, M. Ziosi, and S. Cavicchi. 2007. Fitness variation in response to artificial selection for reduced cell area, cell number and wing area in natural populations of *Drosophila melanogaster*. *BMC Evol. Biol.* 7:S10.
- Vacca, R. A. 2004. Production of reactive oxygen species, alteration of cytosolic ascorbate peroxidase, and impairment of mitochondrial metabolism are early events in heat shock-induced programmed cell death in tobacco bright-yellow 2 cells. *Plant Physiol.* 134:1100–1112.
- Van der Have, T., and G. De Jong. 1996. Adult size in ectotherms: temperature effects on growth and differentiation. *J. Theor. Biol.* 183:329–340.
- Walters, R. J., and M. Hassall. 2006. The temperature-size rule in ectotherms: may a general explanation exist after all? *Am. Nat.* 167:510–523.
- Wickham, H. 2009. *ggplot2: elegant graphics for data analysis*. Springer-Verlag, New York.
- Wickham, H. 2011. The split-apply-combine strategy for data analysis. *J. Stat. Softw.* 40:1–29.
- Woods, H. A. 1999. Egg-mass size and cell size: effects of temperature on oxygen distribution. *Am. Zool.* 39:244–252.

Associate Editor: S. Collins  
Handling Editor: D. W. Hall

## Supporting Information

Additional supporting information may be found online in the Supporting Information section at the end of the article.

**Figure S1.** For all analyses, *Temperature* was treated as a continuous variable (here represented by the continuous lines), but we ensured that treating *Temperature* as a discrete categorical variable (points and point ranges) did not change any of our conclusions.

**Figure S2.** Model fits for the four variables at each size-selection treatment reared at 22°C (usual temperature), 18°C (−4), and 26°C (+4). Each line connects the partial residual of an independent lineage extracted from the best-fitting mixed-effect linear model.

**Figure S3.** Mean cell size monitored during growth trials as a function of temperature (rows) and size-selection treatment (columns).

**Figure S4.** Population intrinsic growth rates were considerably higher at the beginning of the experiment (day 0 to 3) compared to the end (day 3 to 6) across all temperatures (columns), indicating the onset of resource limitation in the cultures.

**Figure S5.** Temperature-dependency between 18 and 26°C among size-selected treatments (x-axis) between resource-replete (from day 0 to day 3) and resource-deplete (from day 3 to day 6) conditions (colours).

**Table S1.** Anova table for the four best-fitting mixed effect models on each demographic parameter.